

Sensor network for dynamic ice-force identification

The Hanko-1 channel marker case study

Nord, Torodd S.; Oiseth, Ole; Petersen, O.W.; Lourens, Eliz-Mari

Publication date

2015

Document Version

Final published version

Published in

Proceedings of the 23rd international conference on port and ocean engineering under arctic conditions, POAC15

Citation (APA)

Nord, T. S., Oiseth, O., Petersen, O. W., & Lourens, E.-M. (2015). Sensor network for dynamic ice-force identification: The Hanko-1 channel marker case study. In K. Hoyland, E. Kim, R. Lubbad, & W. Lu (Eds.), *Proceedings of the 23rd international conference on port and ocean engineering under arctic conditions, POAC15* Lulea University of Technology.

Important note

To cite this publication, please use the final published version (if applicable).
Please check the document version above.

Copyright

Other than for strictly personal use, it is not permitted to download, forward or distribute the text or part of it, without the consent of the author(s) and/or copyright holder(s), unless the work is under an open content license such as Creative Commons.

Takedown policy

Please contact us and provide details if you believe this document breaches copyrights.
We will remove access to the work immediately and investigate your claim.



Sensor network for dynamic ice-force identification: The Hanko-1 channel marker case study

Torodd S. Nord^{1,2}, Ole Øiseth³, Øyvind Wiig Petersen³, Eliz-Mari Lourens⁴

¹ Centre for Sustainable Arctic Marine and Coastal Technology (SAMCoT), Norwegian University of Science and Technology, Trondheim, Norway

² The University Centre in Svalbard (UNIS), Longyearbyen, Spitsbergen

³ Department of Structural Engineering, Norwegian University of Science and Technology, Trondheim, Norway.

⁴ Faculty of Civil Engineering and Geosciences, Delft University of Technology, Delft, the Netherlands.

ABSTRACT

A measurement campaign at the Hanko-1 channel marker in the Gulf of Finland is planned in order to monitor the forces leading to ice-induced vibrations by means of force identification. It is planned to identify the ice forces using a joint input-state estimation algorithm in conjunction with a modally reduced order model. The methodology is presented together with a finite element model and a detailed analysis that determines the optimal sensor network. The novel approach used to determine the optimal response measurement types and locations ensures the identifiability of the dynamic ice forces from only a limited number of sensors and a selection of vibration modes. The optimal sensor locations are discussed in view of specific challenges posed by the arctic environment.

INTRODUCTION

Channel markers and lighthouses are examples of structures that occasionally experience ice-induced vibrations. In order to understand the nature of these vibrations, several full-scale and laboratory campaigns have been performed over the last decades. Frequency lock-in vibrations was reported by Nordlund et al. (1988), Kärnä and Turunen (1989) and Määttänen (2008) at the lowest natural frequency of the channel markers. Several other structures in the Baltic Sea have been monitored using response measurements and in some cases load panels. For a literature survey, see Bjerkås (2006).

The ice forces are measured either directly or reconstructed by means of inverse techniques. Both have their difficulties and the global forces cannot be derived without assumptions: a global force derived from load panels often relies on assumptions of friction and calibration. Furthermore the panels may not cover the full ice-structure interface. Response sensors cost less, both during the installation and the operating phase. The installation is also easier than for the load panels. A set of global forces derived from a model-based inverse technique depends on model assumptions, sensor locations and on the response information. Sensor networks can be difficult to design because the ice-action point may be unknown and time variant. In addition, other sources of ambient vibrations than the ice content may be present in the response data (Brown, 2007).

In-situ observation of the ice conditions, ice properties and other environmental data are often collected to understand more of the extreme ice-load events. The past measurement campaigns in which such amounts of information were collected, were extensive.

In this paper, we recapitulate an existing approach for real-time monitoring of level-ice forces and responses, and apply it to the Hanko-1 Channel edge marker. The objective is to identify the dynamic forces with only a limited number of response measurements.

Both the states (ensemble of displacements and velocities) and the forces will be treated as unknowns and jointly estimated using a finite element model and a joint input-state estimation algorithm. For modally reduced order models, Maes et al. (2014) recently demonstrated sensor network requirements and considerations ensuring force identifiability when using the joint input-state estimation algorithm. In this contribution, these requirements are used to design a sensor network for the Hanko-1 Channel marker.

DUAL FORCE AND STATE ESTIMATION

In this section we describe the system equations, the state-space transform, the joint input-state algorithm, and the requirements for the force identification to succeed.

System equations

The ice force is treated as an unknown concentrated load acting on a linear time-invariant structure that is represented by a finite element model consisting of a limited number of vibrational modes:

$$\ddot{\mathbf{z}}(t) + \mathbf{\Gamma}\dot{\mathbf{z}}(t) + \mathbf{\Omega}^2\mathbf{z}(t) = \mathbf{\Phi}^T\mathbf{S}_p\mathbf{p}(t) \quad (1)$$

where $\mathbf{z}(t) \in \mathbb{R}^{n_m}$ is the vector of modal coordinates and n_m the number of modes used to assemble the model. The force vector $\mathbf{p}(t) \in \mathbb{R}^{n_p}$ is specified to act at the desired locations through the force influence matrix $\mathbf{S}_p \in \mathbb{R}^{n_{\text{DOF}} \times n_p}$, where n_p is the number of force time histories and n_{DOF} is the number of degrees of freedom. $\mathbf{\Gamma} \in \mathbb{R}^{n_m \times n_m}$ is the diagonal damping matrix populated diagonally with the terms $2\xi_j\omega_j$ where ω_j and ξ_j are the natural frequency and damping ratio corresponding to mode j , respectively. $\mathbf{\Omega} \in \mathbb{R}^{n_m \times n_m}$ is a diagonal matrix containing the natural frequencies ω_j and $\mathbf{\Phi} \in \mathbb{R}^{n_{\text{DOF}} \times n_m}$ is a matrix collecting the mass-normalized mode shapes.

State-space model

The continuous-time state vector $\mathbf{x}(t) \in \mathbb{R}^{n_s}$, $n_s = 2n_m$, is defined as follows:

$$\mathbf{x}(t) = \begin{pmatrix} \mathbf{z}(t) \\ \dot{\mathbf{z}}(t) \end{pmatrix} \quad (2)$$

whereby the equation of motion of second order in Eq. (1) can be organized as a first-order continuous-time state equation

$$\dot{\mathbf{x}}(t) = \mathbf{A}_c\mathbf{x}(t) + \mathbf{B}_c\mathbf{p}(t) \quad (3)$$

where the system matrices $\mathbf{A}_c \in \mathbb{R}^{n_s \times n_s}$ and $\mathbf{B}_c \in \mathbb{R}^{n_s \times n_p}$ are defined as

$$\mathbf{A}_c = \begin{bmatrix} \mathbf{0} & \mathbf{I} \\ -\mathbf{\Omega}^2 & -\mathbf{\Gamma} \end{bmatrix}, \mathbf{B}_c = \begin{bmatrix} \mathbf{0} \\ \mathbf{\Phi}^T\mathbf{S}_p \end{bmatrix} \quad (4)$$

The measurements are collected in a data vector $\mathbf{d}(t) \in \mathbb{R}^{n_d}$, in which the observations can be a linear combination of displacement, velocity and acceleration, with n_d the number of data measurements. The data vector is constructed as follows:

$$\mathbf{d}(t) = \mathbf{S}_a \Phi \ddot{\mathbf{z}}(t) + \mathbf{S}_v \Phi \dot{\mathbf{z}}(t) + \mathbf{S}_d \Phi \mathbf{z}(t) \quad (5)$$

where the selection matrices $\mathbf{S}_a, \mathbf{S}_v$ and $\mathbf{S}_d \in \mathbb{R}^{n_d \times n_{\text{DOF}}}$ are populated according to the spatial location at which acceleration, velocity, displacement and/or strain are measured. Eq. (5) can be transformed into state-space form using Eqs. (1) and (2):

$$\mathbf{d}(t) = \mathbf{G}_c \mathbf{x}(t) + \mathbf{J}_c \mathbf{p}(t) \quad (6)$$

where the matrices $\mathbf{G}_c \in \mathbb{R}^{n_d \times n_s}$ and $\mathbf{J}_c \in \mathbb{R}^{n_d \times n_p}$ represent the output influence matrix and direct transmission matrix, respectively, defined as follows:

$$\begin{aligned} \mathbf{G}_c &= [\mathbf{S}_d \Phi - \mathbf{S}_a \Phi \Omega^2 \quad \mathbf{S}_v \Phi - \mathbf{S}_a \Phi \Gamma] \\ \mathbf{J}_c &= [\mathbf{S}_a \Phi \Phi^T \mathbf{S}_p] \end{aligned} \quad (7)$$

In discrete time under a zero-order hold assumption and given a sampling rate of $1/\Delta t$, Eqs. (3) and (6) become:

$$\mathbf{x}_{k+1} = \mathbf{A} \mathbf{x}_k + \mathbf{B} \mathbf{p}_k \quad (8)$$

$$\mathbf{d}_k = \mathbf{G} \mathbf{x}_k + \mathbf{J} \mathbf{p}_k \quad (9)$$

where

$$\mathbf{x}_k = \mathbf{x}(k\Delta t), \mathbf{d}_k = \mathbf{d}(k\Delta t), \mathbf{p}_k = \mathbf{p}(k\Delta t), k = 1, \dots, N$$

and

$$\mathbf{A} = e^{\mathbf{A}_c \Delta t}, \mathbf{B} = [\mathbf{A} - \mathbf{I}] \mathbf{A}_c^{-1} \mathbf{B}_c$$

$$\mathbf{G}_c = \mathbf{G}, \mathbf{J}_c = \mathbf{J}$$

Joint input-state estimation algorithm

With the system matrices $\mathbf{A}, \mathbf{B}, \mathbf{G}$ and \mathbf{J} known, the algorithm developed by Gilljins and De Moor (2007) is used to jointly estimate the forces and states. It has the structure of a Kalman filter, but with the true force replaced with an optimal estimate. Unlike force identification using the traditional Kalman filter (see Lourens et al. (2012b)), no regularization parameter has to be calculated. By introducing the random variables \mathbf{w}_k and \mathbf{v}_k , which represent the stochastic system and measurement noise, respectively, the discrete-time state-space equations become the following:

$$\mathbf{x}_{k+1} = \mathbf{A} \mathbf{x}_k + \mathbf{B} \mathbf{p}_k + \mathbf{w}_k \quad (10)$$

$$\mathbf{d}_k = \mathbf{G} \mathbf{x}_k + \mathbf{J} \mathbf{p}_k + \mathbf{v}_k \quad (11)$$

where it is assumed that the vectors \mathbf{w}_k and \mathbf{v}_k are mutually uncorrelated, zero-mean, white-noise signals with known time invariant covariance matrices $\mathbf{Q} = E\{\mathbf{w}_k \mathbf{w}_k^T\}$ and $\mathbf{R} = E\{\mathbf{v}_k \mathbf{v}_k^T\}$. The algorithm predicts the forces and states in three steps summarized below: the unbiased minimum-variance input estimation (MVU), the measurement update, and the time update.

Input estimation:

$$\tilde{\mathbf{R}}_k = \mathbf{G}\mathbf{P}_{k|k-1}\mathbf{G}^T + \mathbf{R} \quad (12)$$

$$\mathcal{M}_k = (\mathbf{J}^T \tilde{\mathbf{R}}_k^{-1} \mathbf{J})^{-1} \mathbf{J}^T \tilde{\mathbf{R}}_k^{-1} \quad (13)$$

$$\hat{\mathbf{p}}_{k|k} = \mathcal{M}_k (\mathbf{d}_k - \mathbf{G}\hat{\mathbf{x}}_{k|k-1}) \quad (14)$$

$$\mathbf{P}_{p[k|k]} = (\mathbf{J}^T \tilde{\mathbf{R}}_k^{-1} \mathbf{J})^{-1} \quad (15)$$

Measurement update:

$$\mathbf{L}_k = \mathbf{P}_{k|k-1} \mathbf{G}^T \tilde{\mathbf{R}}_k^{-1} \quad (16)$$

$$\hat{\mathbf{x}}_{k|k} = \hat{\mathbf{x}}_{k|k-1} + \mathbf{L}_k (\mathbf{d}_k - \mathbf{G}\hat{\mathbf{x}}_{k|k-1} - \mathbf{J}\hat{\mathbf{p}}_{k|k}) \quad (17)$$

$$\mathbf{P}_{k|k} = \mathbf{P}_{k|k-1} - \mathbf{L}_k (\tilde{\mathbf{R}}_k - \mathbf{J} \mathbf{P}_{p[k|k]} \mathbf{J}^T) \mathbf{L}_k^T \quad (18)$$

$$\mathbf{P}_{xp[k|k]} = \mathbf{P}_{px[k|k]}^T = -\mathbf{L}_k \mathbf{J} \mathbf{P}_{p[k|k]} \quad (19)$$

Time update:

$$\mathbf{x}_{k+1|k} = \mathbf{A}\hat{\mathbf{x}}_{k|k} + \mathbf{B}\hat{\mathbf{p}}_{k|k} \quad (20)$$

$$\mathbf{P}_{k+1|k} = [\mathbf{A} \quad \mathbf{B}] \begin{bmatrix} \mathbf{P}_{k|k} & \mathbf{P}_{xp[k|k]} \\ \mathbf{P}_{px[k|k]} & \mathbf{P}_{p[k|k]} \end{bmatrix} \begin{bmatrix} \mathbf{A}^T \\ \mathbf{B}^T \end{bmatrix} + \mathbf{Q} \quad (21)$$

Error covariance for both the estimated states and forces are obtained in every step and collected in $\mathbf{P}_{k|k} \in \mathbb{R}^{n_s \times n_s}$ and $\mathbf{P}_{p[k|k]} \in \mathbb{R}^{n_p \times n_p}$, respectively. For more details on the algorithm and the assumptions it is based upon, the reader is referred to Lourens et al. (2012a).

A step action table is provided to help implementation of this framework:

1. Model assembly and tuning; extract mass normalized eigenvectors and natural frequencies ($\Phi \in \mathbb{R}^{n_{\text{DOF}} \times n_m}$, $\Omega \in \mathbb{R}^{n_m \times n_m}$).
2. Define force influence locations ($\mathbf{S}_p \in \mathbb{R}^{n_{\text{DOF}} \times n_p}$).
3. Define sensor locations and assemble the data vector.
4. State-space transform.
5. Perform joint state and input estimation.

Requirements for force identification using the JSI algorithm

The correct types and locations of response measurements are essential to successfully identify the forces. Maes et al. (2014) formulated a set of mathematical criteria that can be used to design sensor networks. The criteria ensure that the dynamic forces can be identified using the joint input-state estimation algorithm (Eqs. (10) – (21)) in conjunction with a modally reduced order model (Eqs.(8) – (9)). The first criterion ensures that the ice force can be estimated from the response measurements without a time delay. The second ensures that the stability of the system inversion is maintained. It is recommended for the reader to look into the reference for additional criteria that ensure the complete dynamic response to be identified.

Direct invertibility

It is required that the system input (the ice force) can be estimated from the output without a time delay. This is proven to hold if $\text{rank}(\mathbf{J}) = \text{rank}(\mathbf{S}_a \Phi \Phi^T \mathbf{S}_p) = n_p$. In order to ensure this, first the number of excited modes should be larger or equal to the number of forces, $\text{rank}(\mathbf{S}_p^T \Phi) = n_p$. Second, it is required that at least n_p accelerations are measured to secure a direct coupling between the acceleration responses and the estimated forces. Furthermore, the acceleration measurements should pertain significant contributions from the modes excited by the forces.

Stability requirements

The stability of the system inversion can be checked by investigating the so-called transmission zeros. These depend on the matrices \mathbf{A} , \mathbf{B} , \mathbf{G} and \mathbf{J} , and are found by solving the following eigenvalue problem (Emami-Naeini and Van Dooren, 1982)

$$\begin{bmatrix} \mathbf{A} - \lambda_j \mathbf{I} & \mathbf{B} \\ \mathbf{G} & \mathbf{J} \end{bmatrix} \begin{bmatrix} \mathbf{x}_{[0]} \\ \mathbf{p}_{[0]} \end{bmatrix} = \begin{bmatrix} \mathbf{0} \\ \mathbf{0} \end{bmatrix} \quad (22)$$

where $\lambda_j \in \mathbb{C}$ a finite transmission zero for any selection for the corresponding initial conditions $\mathbf{x}_{[0]} \in \mathbb{C}^{n_s}$ and $\mathbf{p}_{[0]} \in \mathbb{C}^{n_p}$ for the state and force, respectively. If $|\lambda_j| < 1$, the system inversion is stable, while if $|\lambda_j| > 1$ the system inversion is unstable. When $|\lambda_j| = 1$, the system inversion is marginally stable. Maes et al. (2014) explained the 0 Hz marginally stable transmission zero to occur because the acceleration and velocity measurements are insensitive to an excitation which is constant with time. The latter one occurs if only acceleration data is included in the measurement setup. By including displacement/strain measurements one can omit the marginally stable transmission zero at 0 Hz, and the inversion stability can be further checked from $\text{rank}(\mathbf{J} - \mathbf{G}(\mathbf{A} - \mathbf{I})^{-1}\mathbf{B}) = \min(n_p, n_d)$.

FORCE IDENTIFICATION ON THE HANKO-1 CHANNEL MARKER

The Hanko-1 channel marker is located at N59 44.11 and E23 02.36 (WGS-84) offshore the city Hanko in Finland. The structure was chosen because of its location close to the mainland and the fact that earlier measurements showed frequency lock-in vibrations. The foundation pile is molded into the bedrock well by concrete casting (Fig.1). A steel cone supports the 0.8 m diameter circular-sectioned steel superstructure which has varying wall thickness from the mean water level up to the lantern at the top (Fig.2). The structure exhibited frequency lock-in vibrations at the first natural frequency of 4.6 Hz on several occasions. For more information about frequency lock-in vibrations on this channel marker and others, see Määttänen (2008), Kärnä and Turunen (1989) and Nordlund et al. (1988).

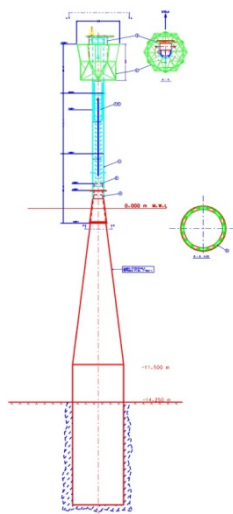


Figure 1. Hanko-1 Channel marker design.



Figure 2. Picture of a typical Channel marker, from Määttänen (2008).

Finite element model

The structure is modelled using quadrilateral finite-membrane-strain shell elements with reduced integration (S4R) in the software ABAQUS. Construction blueprints were used to define the model properties. All the shell degrees of freedom of the model are constrained in the rock well (cf. Fig. 1). The lantern plates were simplified from the true geometry with the total mass kept similar to the real value, ~ 1400 kilograms. The added mass of the displaced water is accounted for through the density of the steel below the mean water level. Several of the vibration modes are symmetric in the x-z direction, with the corresponding natural frequencies up to 40Hz given in Table 1. Circumferential modes are found in the substructure due to the high material density used to account for the displaced water. The bending modes are displayed in Fig. 3, in which the next section will demonstrate why these are important for the assembly of a modally reduced order model.

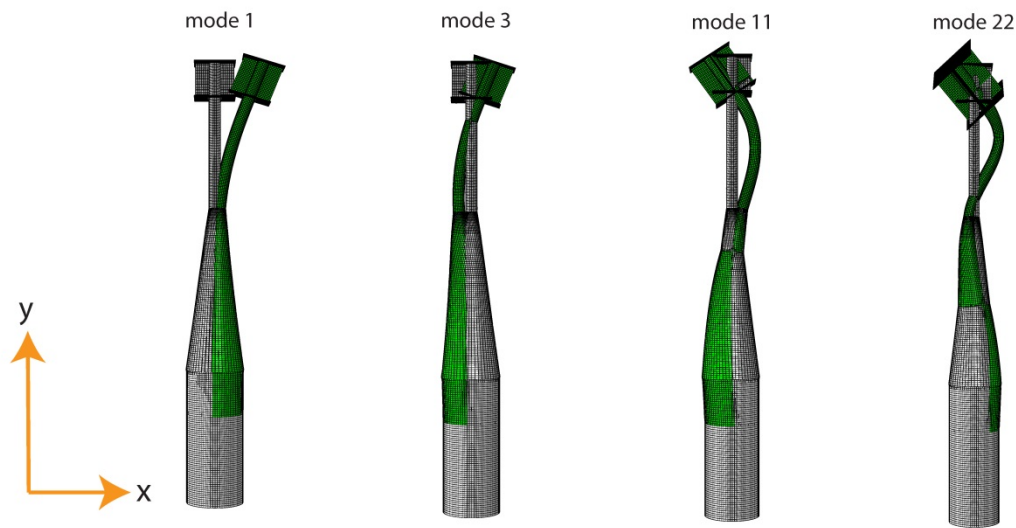


Figure 3. Bending vibration modes of Hanko-1.

Table 1. Finite element model natural frequencies and vibration modes

Mode	$f_j = \frac{\omega_j}{2\pi}$ [Hz]	Mode shape description (<i>displayed modes</i>)
1,2	4.68	<i>Bending mode in x direction (mode 1) and z direction (mode 2)</i>
3,4	9.91	<i>Bending mode in x direction (mode 3) and z direction (mode 4)</i>
5,6	10.55	Circumferential mode in the substructure
7,8	13.68	Circumferential mode in the substructure
9,10	20.15	Circumferential mode in the substructure
11,12	22.12	<i>Bending mode in x direction (mode 11) and z direction (mode 12)</i>
13,14	27.96	Circumferential mode in the substructure
15-18	28.4-29.2	Circumferential mode in the substructure
19	32.95	Torsion
20,21	33.45	Circumferential mode in the substructure
22,23	35.16	<i>Bending modes 45 degree to the principal axes</i>
24	40.72	Circumferential mode in the substructure

Direct invertibility

The locations at which each accelerometers are placed have an effect on the direct invertibility. 13 possible accelerometer locations and two assumed attack points for the ice forces are displayed in Fig. 4 (a). The modal influences, $\mathbf{S}_p^T \Phi$, of the two assumed force locations in Fig.4 (a) are shown in Fig. 4 (b) (top). The force locations have a significant influence on the modes 1, 2, 3, 4, 11, 12, 22 and 23, which means that if the global forces in x and z directions are sought, respectively, $n_p = 2$ and $\mathbf{S}_p^T \Phi$ will be of full rank.

The contribution from the modes to each of the possible accelerometer locations, $\mathbf{S}_a \Phi$, are displayed in Fig. 4 (b) (bottom). At least two accelerometers are required in order to assure that $\text{rank}(\mathbf{J}) = n_p = 2$. In addition, it is assumed that four extra accelerometers are available providing extra safety for the measurements in case some accelerometers malfunction. The d_1, d_2, d_3, d_6, d_7 and d_8 locations capture a significant influence through all the bending modes (cf. Fig. 3) which also have a significant influence from the input.

At some locations the major modal contributions cancel each other out: d_5 is a location at which an appropriate force influence and modal contribution from several modes are obtained (Fig. 4b), but with a low direct transmission value, $\mathbf{S}_a \Phi \Phi^T \mathbf{S}_p$ (Fig 5). The low transmission value means that the point has a weak input-output coupling, therewith not a preferred location for an accelerometer. The strongest input-output coupling is found slightly above the ice-action point.

Assuming that the inside of the structure is inaccessible, the sensors must be located on the outer surface. If the sensors are deployed too close to the ice-action point, they also become vulnerable to the ice floe. Therefore it is assumed that the sensors cannot be mounted closer than 1 meter from the ice-action point. Variation in the ice-action point can occur due to water-level fluctuations, interaction with deformed ice, such as rafted ice, ridged ice etc. In order to find the optimal accelerometer locations and account for varying attack-point, one can also effectively assemble in a similar manner as was done above for only two locations, a larger vector, \mathbf{S}_p , of all possible force locations and vary the sensor positions, \mathbf{S}_a .

The location d_10 is the lowermost possible accelerometer location which gives the best input-output coupling, and the locations below that level are not practical alternatives despite of their strong input-output coupling. The third and fourth accelerometer could for instance be installed at locations d_8, such that if the lowermost fails, a strong input-output coupling is still maintained. Location d_3 is a suitable location for the fifth and sixth accelerometer.

The modes which insignificantly contribute to the response, or have an insignificant force influence, are primarily circumferential modes of the substructure. These may be inaccurately described by the added mass and therefore they may bring large modelling errors into the system. Because of their small contribution to the response, these may also lead to a numerically rank-deficient modal projection sensor selection matrix, $\mathbf{S}_a \Phi$, (van der Male and Lourens, 2015). Hence, the modally reduced order model that will be used throughout this paper retains only the modes 1, 2, 3, 4, 11, 12, 22 and 23. A set of system matrices \mathbf{A} , \mathbf{B} , \mathbf{G} and \mathbf{J} are obtained using these eight modes and the six chosen accelerometer locations above. To ensure that sufficient numerical rank is obtained, the singular values of \mathbf{J} are calculated. Two positive singular values of $7.333 \cdot 10^{-5}$ and $7.3184 \cdot 10^{-5}$ were found, hence $\text{rank}(\mathbf{J}) = n_p = 2$.

Note that because the excluded modes only contributed marginally to the input-output coupling, Fig. 5 remained almost unchanged with the modally reduced order model with $n_m = 8$.

Stability requirements

The chosen accelerometer installations, the modally reduced order model with $n_m = 8$ and a sampling frequency of 100Hz rendered no unstable transmission zeros. However, the system inversion will only be marginally stable due to the lack of information at 0 Hz and the singular values of the matrix $\mathbf{J} - \mathbf{G}(\mathbf{A} - \mathbf{I})^{-1}\mathbf{B}$ were $2.3050 \cdot 10^{-20}$ and $1.3968 \cdot 10^{-20}$. In practice, to ensure that the solution is stabilized the singular values should be larger, otherwise the numerical rank falsely suggests sufficient stability is fulfilled.

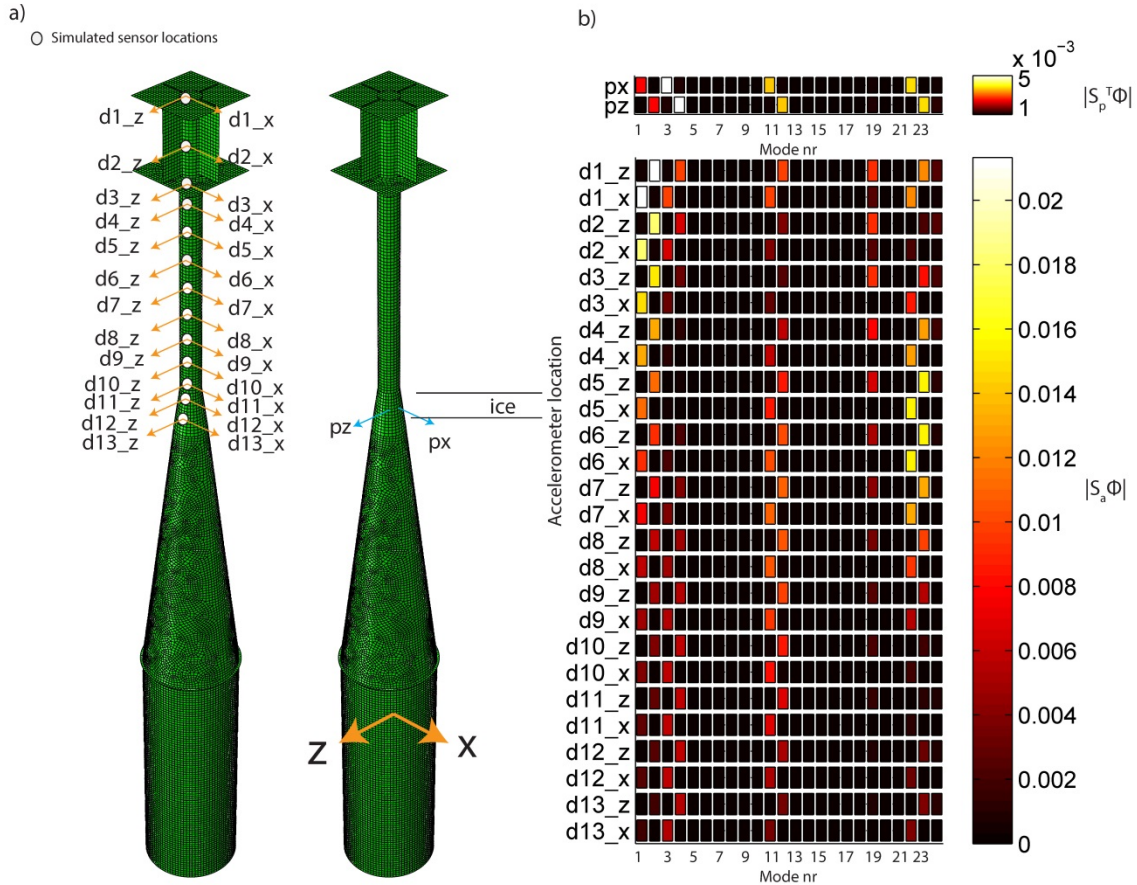


Figure 4. a) simulated sensor locations b) modal influences of forces and accelerations at simulated locations.

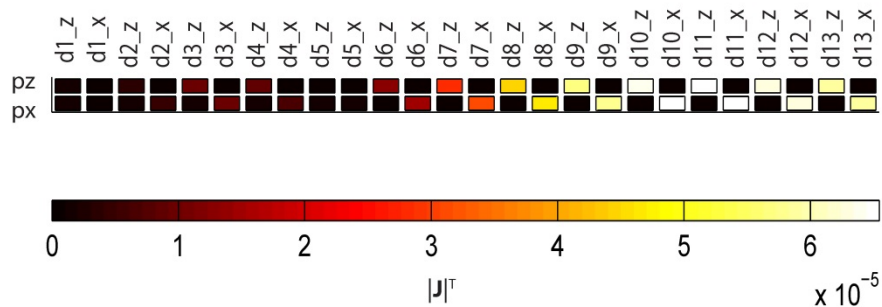


Figure 5. Direct transmission value, \mathbf{J} , as function of accelerometer location.

Strain measurements are one way to eliminate the marginally stable transmission zeros. The strain gauges should be installed such that the measurement data have contributions from at least $n_p = 2$ modes excited by the unknown forces. Using the modally reduced order model, the modal influences of the bending strains along the locations in Fig 4 (a) are shown in Fig. 6. The corresponding finite elements at each location are taken close to the principal axes on the cross section (Fig. 7), where the bending strains have either full or zero influence for vibration modes parallel or perpendicular to the principal axes. Locations e_3, down to e_7 show good strain influence through several modes. Because each location should capture bending strain in both the xy and zy plane, two active strain gauges at for instance the level e_4 would ensure both to be captured.

Since the system matrices depend on the modal properties, the time discretization, the type of sensors and their locations $\mathbf{S}_a, \mathbf{S}_v$ and $\mathbf{S}_d \in \mathbb{R}^{n_d \times n_{\text{DOF}}}$, each alternative for a complete sensor network has to be checked. The inversion stability is now checked for a sensor network that includes the two strain gauges at e_4 and the six accelerometers at locations d_3, d_8 and d_10. Two positive singular values were found from the matrix $\mathbf{J} - \mathbf{G}(\mathbf{A} - \mathbf{I})^{-1}\mathbf{B}$ to be $1.5773 \cdot 10^{-11}$ and $8.4806 \cdot 10^{-12}$, which means that $\text{rank}(\mathbf{J} - \mathbf{G}(\mathbf{A} - \mathbf{I})^{-1}\mathbf{B}) = 2 = n_p$. Hence the marginally stable transmission zeros are eliminated and since the system had no unstable transmission zeros, stable inversion is provided.

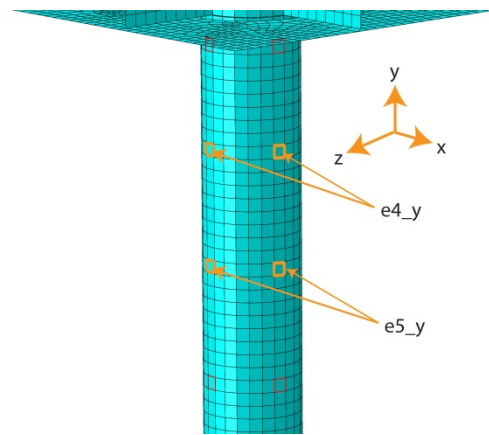
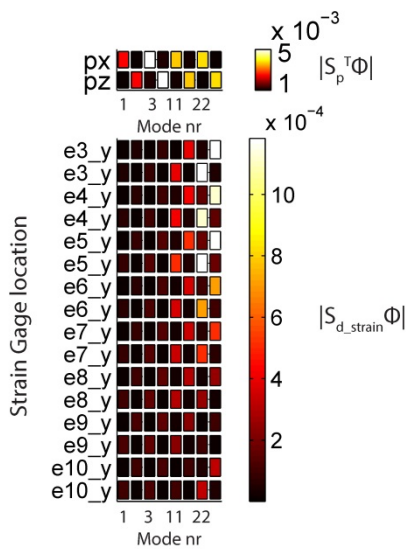


Figure 6. Modal influence on strains at different spatial locations.

Figure 7. Two elements at each spatial level used to simulate the modal strain influence.

Static force component

Continuous ice crushing causes both static and dynamic forces, and the sensor network described above is valid only for identification the dynamic forces. Because the simulated strain gauge locations are above the ice-action point, they provide no information about the static content of the ice force. An optimal solution includes strain gauges installed below the mean water-level, similar to the instrumentation Turunen and Nordlund (1988) presented on a channel marker. Biaxial inclinometer/tiltmeter could also provide the static response. Such response sensors were installed to reconstruct the forces on the Confederation Bridge (Brown, 2007) and the Nordströmsgrund lighthouse (Frederking, 2005). Whereas both the static and

dynamic part of the forces and states will be identified simultaneously with the proposed algorithm, it is essential that the inclinometer/tiltmeter can provide accurate measurements also in the dynamic range. If not, the inclinometer/tiltmeter response may distort the identified forces. In addition, some structures are prone to lateral deformations in the soil due to the ice action and hence the inclination/tilt may be an inaccurate means to obtain the static forces.

DISCUSSION

The joint input-state estimation algorithm has become a tool for force and response estimation with well-developed requirements, first the truncation to reduced order systems by Lourens et al. (2012a) and second a compilation of requirements for a stable inversion by Maes et al. (2014). Recent papers (Nord et al., 2014; Nord et al., 2015) also successfully applied this framework to identify level-ice forces on a laboratory structure.

With the conditions described in this paper met, the algorithm will render the ice forces from the measured signals. The presented results are obtained from a model that contains several assumptions, such as the superstructure mass and the boundary conditions used in the foundation. Static and dynamic calibrations can be used to tune the model properties and provide more accurate results.

CONCLUSION

A sensor network consisting of accelerometers and strain gages are suggested in order to identify ice forces on the Hanko-1 channel marker. The network ensures the identifiability of dynamic ice forces using the joint input-state estimation algorithm in conjunction with a modally reduced order model.

ACKNOWLEDGEMENTS

The authors wish to acknowledge the support of the Research Council of Norway through the Centre for Research-based Innovation SAMCoT, and the support of all SAMCoT partners. The authors also acknowledge Professor Emeritus Mauri Määtänen for providing information on sensor installations in arctic waters, the structural design and dynamic behaviour of the Finnish channel edge markers.

REFERENCES

- Bjerkås, M., 2006. Ice action on offshore structures. PhD Thesis, NTNU, ISBN 82-471-7756-0, 173 pp.
- Brown, T.G., 2007. Analysis of ice event loads derived from structural response. *Cold Regions Science and Technology*, 47(3): 224-232.
- Emami-Naeini, A. and Van Dooren, P., 1982. Computation of zeros of linear multivariable systems. *Automatica*, 18(4): 415-430.
- Frederking, R., 2005. Tiltmeter application at Nordströmsgrund lighthouse- Strice Project, 18th International Conference on Port and Ocean Engineering Under Arctic Conditions pp. 399-408.
- Gillijns, S. and De Moor, B., 2007. Unbiased minimum-variance input and state estimation for linear discrete-time systems with direct feedthrough. *Automatica*, 43(5): pp. 934-937.
- Kärnä, T. and Turunen, R., 1989. Dynamic response of narrow structures to ice crushing. *Cold Regions Science and Technology*, 17(2): 173-187.
- Lourens, E., Papadimitriou, C., Gillijns, S., Reynders, E., De Roeck, G. and Lombaert, G., 2012a. Joint input-response estimation for structural systems based on reduced-order

- models and vibration data from a limited number of sensors. *Mechanical Systems and Signal Processing*, 29(0): pp. 310-327.
- Lourens, E., Reynders, E., De Roeck, G., Degrande, G. and Lombaert, G., 2012b. An augmented Kalman filter for force identification in structural dynamics. *Mechanical Systems and Signal Processing*, 27(0): 446-460.
- Maes, K., Lourens, E., Van Nimmen, K., Reynders, E., De Roeck, G. and Lombaert, G., 2014. Design of sensor networks for instantaneous inversion of modally reduced order models in structural dynamics. *Mechanical Systems and Signal Processing*(0).
- Määttänen, M., 2008. Ice velocity limit to frequency lock-in vibrations, *International symposium on Ice, IAHR, Vancouver, Canada*, pp. 1265-1276.
- Nord, T.S., Lourens, E.-M., Øiseth, O. and Metrikine, A., 2014. Model-based force identification in experimental ice-structure interaction by means of Kalman filtering, *EURODYN, Porto, Portugal*.
- Nord, T.S., Lourens, E.-M., Øiseth, O. and Metrikine, A., 2015. Model-based force and state estimation in experimental ice-induced vibrations by means of Kalman filtering. *Cold Regions Science and Technology*, 111(0): pp. 13-26.
- Nordlund, O.P., Tuomo, K. and Järvinen, E., 1988. Measurements of ice-induced vibrations of channel markers, *IAHR Ice Symposium, Sapporo, Japan*, pp. 537-548.
- Turunen, R. and Nordlund, O.-P., 1988. Full-scale measurements of the dynamic properties of a channel marker, *IAHR Ice Symposium, Sapporo, Japan*, pp. 549-560.
- van der Male, P. and Lourens, E.-M., 2015. Operational Vibration-Based Response Estimation of Offshore wind Lattice Structures, *IMAC XXXIII A Conference and Exposition on Structural Dynamics, Paper no. 198, Orlando, Florida, US*.